iScience

Article

Fact or fiction: What is in your $^{15}N_2$ and $^{15}NH_3$ cylinders for sustainable ammonia and urea research?

Graphical abstract

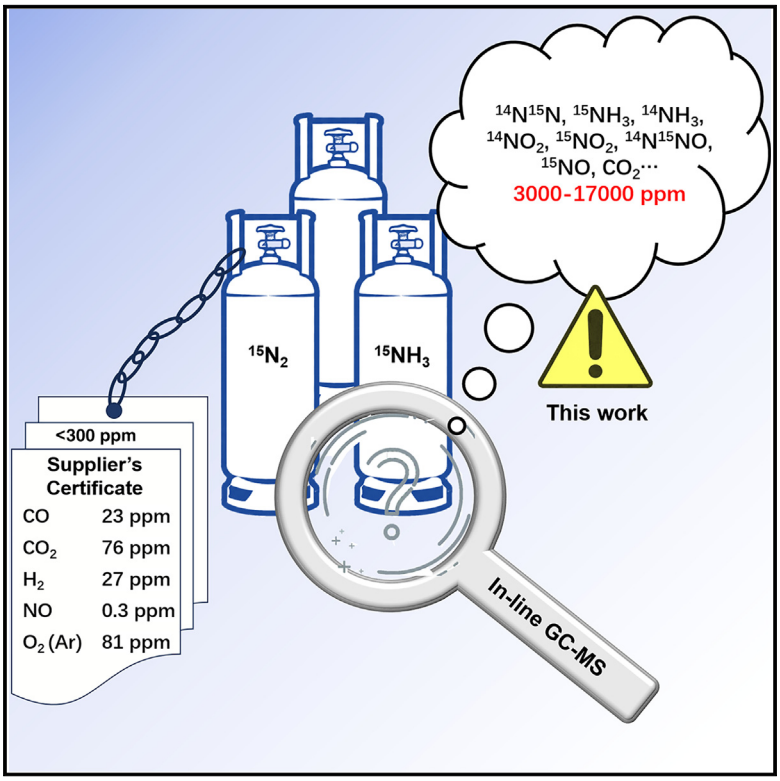

Highlights

- An in-line GC-MS method is developed to test impurities in $^{15}N_2$ and $^{15}NH_3$
- High concentrations of $^{15}NH_3$, $^{15}N^{14}N$, and $^{15}NO_x$ impurities are confirmed
- Recommended protocols have been formed to eliminate false positives

Authors

Sanli Tang, Chengliang Mao, Guanshu Zhao, Jessica Ye, Wenqiang Qu, Lei Wu, Geoffrey Ozin

Correspondence

chengliang.mao@sjtu.edu.cn (C.M.), g.ozin@utoronto.ca (G.O.)

In brief

Environmental chemical engineering; Organic reaction; Green chemistry

Tang et al., 2025, iScience *28*, 112072
April 18, 2025
https://doi.org/10.1016/j.isci.2025.112072

CellPress

iScience

CellPress
OPEN ACCESS

Article

Fact or fiction: What is in your $^{15}N_2$ and $^{15}NH_3$ cylinders for sustainable ammonia and urea research?

Sanli Tang,[1,4] Chengliang Mao,[2,3,4,*] Guanshu Zhao,[2] Jessica Ye,[2] Wenqiang Qu,[2] Lei Wu,[2] and Geoffrey Ozin[2,5,*]
[1]Institute of Engineering Thermophysics, Chinese Academy of Sciences, Beijing 100190, China
[2]Solar Fuels Group, Department of Chemistry, University of Toronto, 80 St. George Street, Toronto, ON M5S 3H6, Canada
[3]School of Environmental Science and Engineering, Shanghai Jiao Tong University, Shanghai 200240, China
[4]These authors contributed equally
[5]Lead contact
*Correspondence: chengliang.mao@sjtu.edu.cn (C.M.), g.ozin@utoronto.ca (G.O.)
https://doi.org/10.1016/j.isci.2025.112072

SUMMARY

Attaining reliable performance indicators via ^{15}N-labeling is a daunting research endeavor for sustainable ammonia and urea synthesis processes, as currently obtained reaction rates and yields are often low. However, artifact and misinterpretation can be induced by ppm-level impurities in commercial $^{15}N_2$ and $^{15}NH_3$ cylinders, which are not well understood. Here, we report quantitative in-line gas chromatography-mass spectrometry (GC-MS) analysis of impurities in commercial $^{15}N_2$ and $^{15}NH_3$ cylinders at ppm level, in conjunction with ^{1}H-NMR methods, exemplified by 808–16,252 ppm of $^{14}N^{15}N$, 0–4,891 ppm $^{15}NH_3$, 3–319 ppm $^{14}NH_3$, 0–231 ppm of $^{14}NO_2$, 0–176 ppm $^{15}NO_2$, and 0–566 ppm $^{15}N^{16}O$ impurities, some of which were not reported in cylinder certification nor previous studies. The collected results have formed recommended protocols applicable to all future ^{15}N labeling experiments intended to eliminate false positives.

INTRODUCTION

In a global transition to net-zero, the nitrogen-related chemical transformations have gained great attention.[1,2] Highlighted reactions are ammonia production from the air-abundant molecular dinitrogen (N_2) and its subsequent transformations to all nitrogen-containing chemicals.[3,4] Current fossil-powered industrial ammonia synthesis accounts for 1.6% of global greenhouse gas (GHG) emissions. Decarbonization of this process would allow ammonia to be a viable green hydrogen carrier. Furthermore, green ammonia can react with CO_2 to produce carbon-negative urea, the major nitrogen fertilizer.[1,5]

Among fundamental research aiming to decarbonize these ammonia and urea processes, the use of isotopic gases, particularly $^{15}N_2$ and $^{15}NH_3$, has surged.[6–8] These isotopes contain ^{15}N nucleus (spin = ½; natural abundance: 0.00337, 0.00422), which possesses the same number of protons but differs in the number of neutrons compared to ^{14}N nucleus (spin = 1; natural abundance: 0.99578, 0.99663).[7] This distinction offers an ideal way to trace the nitrogen source of observed products in low-yield laboratory-scale ammonia or urea synthesis experiments down to parts-per-billion level in solution or gaseous phase. This is useful because any nitrogen residues in surrounding environment, such as materials, solution, or container used, and even the gas exhaled by humans, may yield artifacts.[6,9–12] Additionally, ^{15}N isotopes help elucidate reaction pathways and mechanisms by participating in reactions as components of easily detectable intermediates and through kinetic isotope effect (KIE) studies.

$^{15}N_2$ gas cylinders are usually produced by two methods that can form ^{15}N-enriched by-products. The first method is the catalytic dissociation of $^{15}NH_3$ gas over cupric oxide, and the other is the oxidation of $(^{15}NH_4)_2SO_4$ or $^{15}NH_4Cl$ with oxidizing agents such as NaOBr and LiOBr.[13–15] Both methods produce minor amounts of $^{15}NO_x$ (^{15}NO and $^{15}NO_2$) and $^{15}N_2O$ and leave unreacted $^{15}NH_3$, which needs to be removed by bubbling through various alkaline or acidic solutions. During the process, whether those impurities can be thoroughly removed remains unknown, and external contaminations may also be introduced from surroundings. In 2014, a pioneering study indicated that commercial $^{15}N_2$ cylinders (>98% purity, Sigma) contained 2,528 ppm of residues such as ^{15}N-nitrate/nitrite,$^{15}NO_x$ and $^{15}N_2O$, and $^{15}NH_3$ by detecting the absorbing/equilibrating aqueous solutions of natural abundance ammonium and nitrate salts through isotope ratio mass spectrometry (MS).[13] These residues are the products of N_2 fixation reactions and thus sparked concern regarding the reliability of previous $^{15}N_2$ studies utilized in ammonia synthesis research. Though one recent study has confirmed that zero ^{15}N residues were found in absorbing solution after purging the commercial $^{15}N_2$ cylinder gas through a Cu impurity trap (Cu-Zn-Al oxide catalyst),[10] the exact residues in commercial $^{15}N_2$ cylinder remain unknown.

Herein, we utilized an in-line gas chromatography-mass spectrometry (GC-MS) system to unequivocally detect residues in

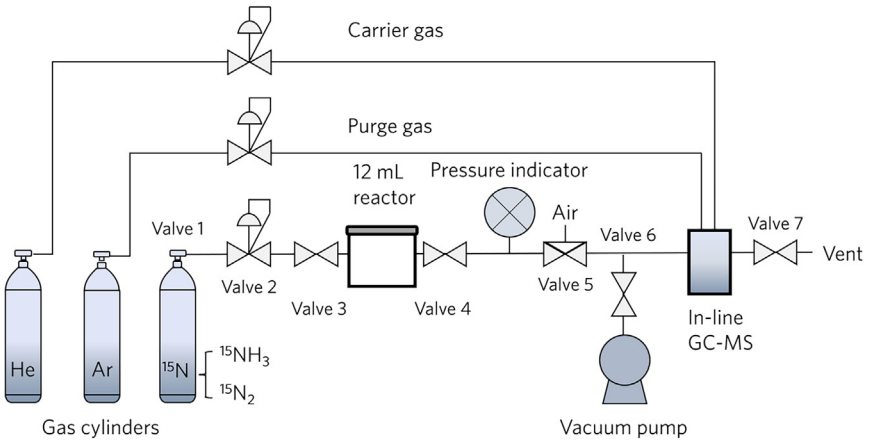

Scheme 1. Schematic of the setup that includes targeted ^{15}N-cylinders, an in-line batch-mode GC-MS analysis system, and a vacuum gas transfer line in between

$^{15}N_2$ cylinders as well as a $^{15}NH_3$ cylinder. Distinct from previous offline methods, our in-line method avoids possible impurities from surroundings, and does not require external D_2O or organic reagents for ^{15}N detections. Besides all possible ^{15}N- and ^{14}N-residues, our method also checks possible CO, CO_2, and hydrocarbons residues. In addition, we used a proton nuclear magnetic resonance (^{1}H-NMR) quantification technique to resolve the insensitivity of our GC-MS method toward the $^{15}NH_3$ residue. Thus, our study is expected to supplement prevailing residue detection methodologies by offering high efficiency, reliability, and cost-effectiveness, and may have broad impacts on fundamental studies of all chemical transformations in the earth's nitrogen cycle.

RESULTS AND DISCUSSION

Residues monitored and detected include N_2, H_2O, O_2, NO, NO_2, N_2O, CO, CO_2, NH_3, and hydrocarbons

The isotope gas cylinder was connected to the GC-MS via a vacuum-involved gas transfer line, which is termed the in-line mode, therefore eliminating contaminations from room air, syringe, and sampling valve (Scheme 1). The gas was sucked into the GC column quantitatively through the negative pressure created by the vacuum pump and the automatic gas sampling valve. He and Ar were used for carrier and purging gas for the GC-MS, respectively.

Total ion chromatogram (TIC) of the Sigma 99% $^{15}N_2$ cylinder gas showed a strong peak at the retention time of 7.3 min using the *C1* method (see STAR Methods for details; Figure 1A). Corresponding extracted ion chromatograms (EICs) demonstrated strong m/z = 15, 30 peaks and weak, but clear, m/z = 28, 31 peaks indicative of $^{15}N_2$ with minor $^{14}N_2$ and $^{15}N^{16}O$ components (Figure 1B). The $^{15}N_2$ assignment was confirmed by an intensity ratio of 11 : 100 between m/z = 15 and m/z = 30 (Figure 1C), which is close to the theoretic $^{15}N/^{15}N_2$ MS intensity ratio (14 : 100).

When the GC-MS spectra were zoomed in, tiny peaks could be observed at 4.2, 4.4, 6.7, 7.2, 7.3, and 7.4 min for the Sigma 99% $^{15}N_2$ cylinder gas (Figure 1B). EIC peaks at 6.7 min were confirmed to be $^{16}O_2$ at (m/z = 16 and 32), while that at 7.2–7.4 min were confirmed as $^{14}N^{15}N^{16}O$ (m/z = 14, 15, and 45), $^{15}N^{16}O$ (m/z = 15, 16, and 31), and $^{14}N^{15}N$ (m/z = 14, 15, and 29), respectively. Peaks at 4.2 and 4.4 min were associated with multiple co-eluted components including CO_2, $^{14}NO_2$, $^{15}NO_2$, $H^{14}NO_2$, $H_2{}^{14}NO_2$, and $H^{15}NO_2$. In addition, the commonly suspected gas residues such as CO and CH_4 in the commercial cylinder were not detected; they would have been present at 8.3 and 10.9 min, respectively (Figure S1).

The peak at 4.2 min was initially but erroneously assigned to CO_2 upon comparison to our CO_2 gas standard, with MS patterns of m/z = 12, 22, 28, and 44–46 when background signals from the H_2O (m/z = 16–20), $^{16}O_2$ (m/z = 16 and 32), and $^{14}N_2$ (m/z = 14 and 28) from leaks in MS and residual Ar purge gas (m/z = 40) were disregarded. Interestingly, the peak at 4.2 min for Sigma 99% $^{15}N_2$ had MS patterns with relative intensities of 100 : 2.7 : 53.9 : 0.9 : 10.7 for m/z = 44, 45, 46, 47, and 48. This was quite different from m/z spectra of our CO_2 standard gas of 100 : 1.25 : 0.4 for m/z = 44, 45, and 46, respectively (Figures 1D and S2). In addition, these values did not match the theoretical ratios for CO_2 of isotopic natural abundance (INA), which is 100 (m/z = 44; $^{12}C^{16}O_2$) : 1.3 (m/z = 45; $^{13}C^{16}O_2$) : 0.4 (m/z = 46; $^{12}C^{16}O^{18}O$).[16] Instead, the significantly enriched m/z = 14 (N fragment), 30 (NO fragment), 46 ($^{14}NO_2$), 47 (isotopic or protonated NO_2) and 48 (isotopic or protonated NO_2) intensities indicate the co-eluted to be $^{14}NO_2$. Given that INA of $^{14}NO_2$ should yield an m/z fragmentation ratio of 9.6 : 100 : 37 : 0.1 for m/z = 14, 30, 46, 47, respectively, and the lack of m/z = 15 (^{15}N fragment) in the peak at 4.2 min, the contaminants were identified as $^{14}NO_2$, $H^{14}NO_2$ and $H_2{}^{14}NO_2$. Furthermore, it is possible that $^{14}N^{16}O^{18}O$ also exists in the cylinder, but this unfortunately cannot be confirmed as signal at m/z = 18 was covered by background signals from H_2O (H_2O at INA should have an EIC ratio of 0.3 : 0.5 : 100 : 21 : 0.9 for m/z = 20, 19, 18, 17, 16, respectively).

The effluents at 4.4 min were assigned to be $^{14}NO_2$, $^{15}NO_2$, and its protonated species according to the presence of m/z = 14, 15, 46, 47, and 48 bands. This is concluded by several steps. First, a lack of m/z = 12 and 13 ($^{12}C/^{13}C$ fragments) suggest these MS patterns do not contain carbon (Figure 1E). Instead, clear but weak m/z = 14 and 15 bands with a relative intensity ratio of 3.2 : 5.5 were observed, indicating the presence of ^{14}N and ^{15}N. Thus, the m/z = 46 and 47 could be assigned to $^{14}NO_2$ and $^{15}NO_2$, respectively. However, the unusually high relative intensity ratio of 100 : 56.7 between m/z = 48 and m/z = 46 indicates that m/z = 48 was not INA of NO_2,[16] but was instead due to protonated $^{14}NO_2$ ($H_2{}^{14}NO_2$) and/or $^{15}NO_2$ ($H^{15}NO_2$).

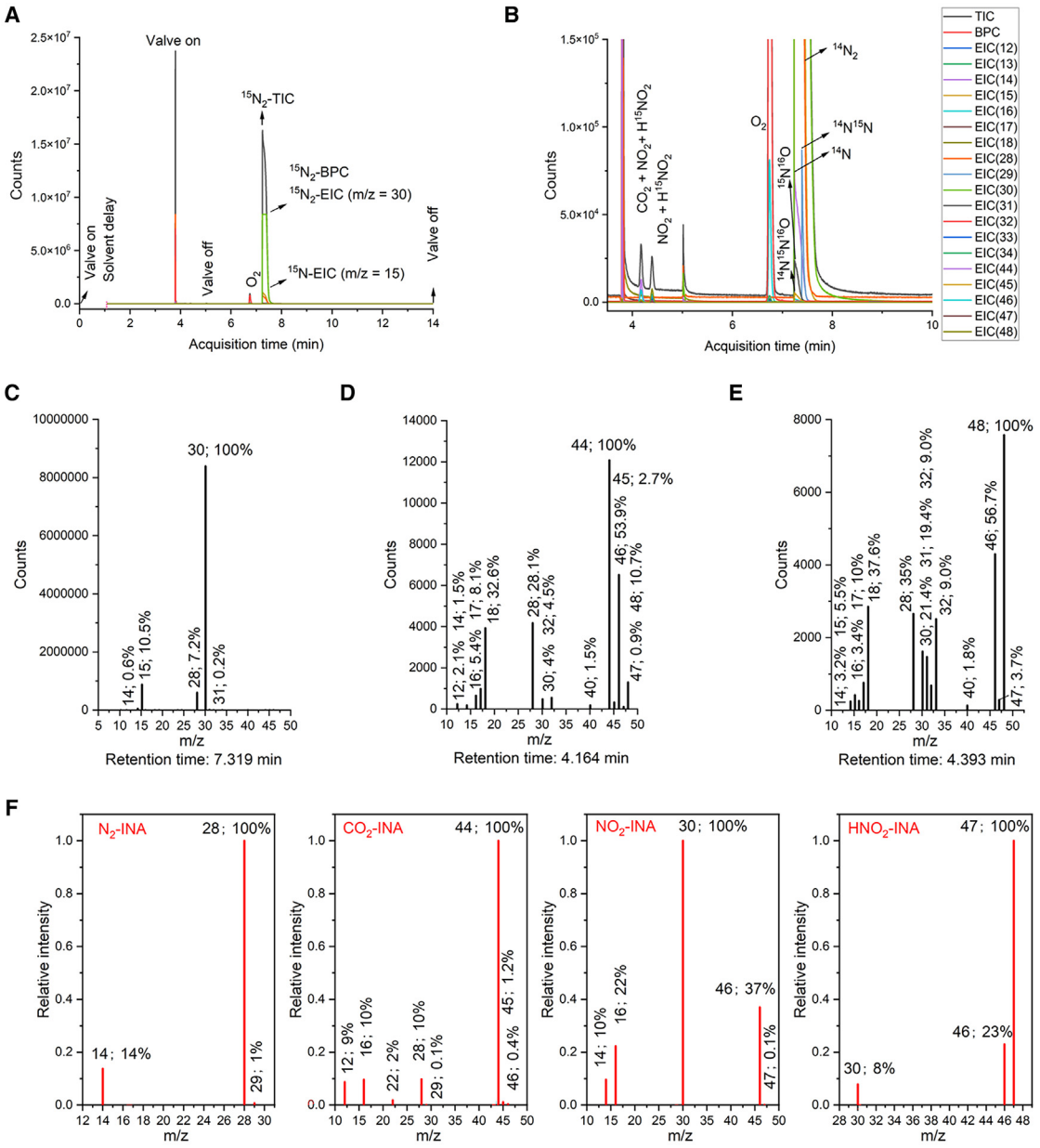

Figure 1. GC-MS spectra of the Sigma 99% $^{15}N_2$ cylinder gas

(A–E) (A) TIC, EIC, and BPC (base peak chromatogram) spectra, (B) selected region at 3.5–10 min, and corresponding (C–E) MS patterns at the retention time of 7.3 ($^{15}N_2$+$^{15}N^{16}O$+$^{14}N_2$), 4.2 (CO_2+$^{14}NO_2$+$H_2{}^{14}NO_2$), and 4.4 ($^{14}NO_2$+$^{15}NO_2$+$H^{15}NO_2$) min, respectively.

(F) Standard or predicted MS patterns of N_2, CO_2, NO_2, and HNO_2 of isotope natural abundance (INA), with dominating ^{1}H, ^{12}C, ^{14}N, and ^{16}O elements. See also Figures S1–S3.

No residual hydrocarbons could be detected for the Sigma 99% $^{15}N_2$ cylinder gas using the *Cn* method and only CO_2 and NO_2 peaks were observed, which was consistent with the results obtained from the *C1* method (see STAR Methods for details; Figure S3). Sigma 98% and Aladdin 99% $^{15}N_2$ cylinder gases were examined using the same procedures (Figures 2A–2C). To our surprise, the $^{15}NO_2$ and related $H^{15}NO_2$ residues observed in the Sigma 99% $^{15}N_2$ cylinder were not detected in either Sigma 98% $^{15}N_2$ 1L or 5L cylinders. However, CO_2, $^{14}NO_2$, $^{15}N^{16}O$, and $^{14}N^{15}N$ residues remained (Figures 2D–2G). In comparison, Aladdin 99% $^{15}N_2$ had CO_2, $^{14}NO_2$, and $^{14}N^{15}N$, but no ^{15}N-related NO_x. However, it should be noted that manual injection of Aladdin 99% $^{15}N_2$ from a gas bag caused slight changes in the retention time for all effluents, as demonstrated by tailing and small shoulder peaks (Figure 2C). Furthermore, it cannot be concluded whether the detected CO_2 was a residue or air leak due to the manual gas sampling.

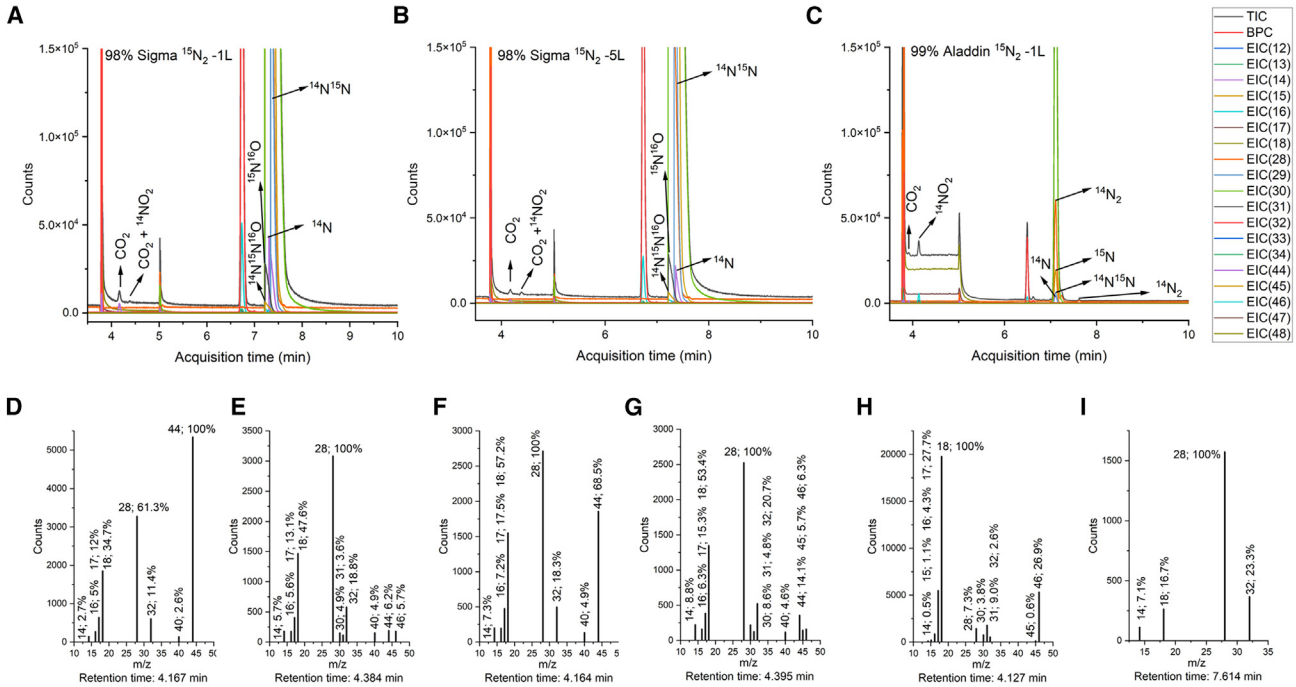

Figure 2. GC-MS spectra of the Sigma 98% $^{15}N_2$ and Aladdin 99% $^{15}N_2$ cylinder gases

TIC, BPC, EIC, and corresponding MS spectra of, (A), (D), (E), Sigma 98% $^{15}N_2$ (1L); (B), (F), (G), Sigma 98% $^{15}N_2$ (5L); and (C), (H), (I), Aladdin 99% $^{15}N_2$. See also Figures S4 and S5.

After checking the NO_x, CO_x, and hydrocarbon residues, we also try to identify NH_3 residues via the *Cn* method of the in-line GC-MS. Unfortunately, due to m/z = 16, 17, and 18 ions of ammonia overlap with fragments of the background water, and the MS signal intensities of residual ammonia are too weak to allow the relative abundance analysis of constituting m/z patterns, ammonia cannot be distinguished from intense water signals by GC-MS (Figure S4). Given a few studies ranging from year 2014 to very recent have continuously reported the $^{15}NH_3$ residues in commercial Sigma cylinders at unacceptable levels,[13,17,18] we double-checked the ammonia via a sensitive quantitative ^{1}H-NMR method as described in our previous work (Figure 3A).[8] The residual $^{15}NH_3$ and $^{14}NH_3$ were confirmed by the characteristic doublet (chemical shift of δ^1H = 6.83 and 6.93 ppm) and triplet (chemical shift of δ^1H = 6.81, 6.88, and 6.96 ppm), respectively. Note this ppm is a unit transformed from the chemical shift in Hertz, followed by dividing it by the frequency rating of the NMR spectrometer and multiplying it by one million. It is different from other ppm as mentioned in this work that indicates the gas concentration, though also called as parts-per-million. Based on the standard curve built through NH_4Cl solution, the concentrations of $^{14}NH_3$ and $^{15}NH_3$ residues were 108–319 and 2,472–4,891 ppm in the 5L 98% Sigma gas cylinder, while no $^{15}NH_3$ could be detected in the 1L 99% Aladdin gas bag, with its $^{14}NH_3$ of similar concentration (10 ppm) to the background ammonia (7 ppm from ambient air, chemicals and materials used during the NMR measurement; Figure 3B).

Residues in the $^{15}NH_3$ gas cylinder were identified to be CO_2 (m/z = 44; 4.2 and 6.7 min), $^{14}N_2O$ (m/z = 44 and 30; 4.4 min), $^{14}N^{16}O$ (m/z = 30; 6.7 min), $^{15}N^{16}O$ (m/z = 31; 6.7 min), and likely $^{14}NH_4OH$ (m/z = 34; 6.7 min; low confidence[16]) using both *C1* and *Cn* methods (Figures 3C–3G).

Comparison of detected residues with supplier's certificates

Listed in the following is the comparison between detected residues and suppliers' certification (Table 1). We noticed that there were significant differences between suppliers' certification and detected components in this work. For example, our Sigma 99% $^{15}N_2$ cylinder gas was purchased in 2022, and its certificate indicated residues of 23 ppm CO, 76 ppm CO_2, 27 ppm H_2, 0.3 ppm NO, and 81 ppm O_2. However, our results showed no CO (high confidence) and some observed residues were not mentioned, including 808 ppm of $^{14}N^{15}N$, 176 ppm of $^{15}NO_2$ (including protonated $H^{15}NO_2$ and potential $H_2{}^{14}NO_2$), 231 ppm of $^{14}NO_2$, 501 ppm $^{15}N^{16}O$, and noticeable $^{14}N^{15}NO$. Similar distinctions were also observed for Sigma 98% $^{15}N_2$ and $^{15}NH_3$ cylinder gas. A certificate was not found for the Aladdin 99% $^{15}N_2$. However, our GC-MS results suggested high-concentrations of $^{14}N^{15}N$ (16252 ppm) and no ^{15}N-enriched NO_x residues.

Significance and potential of findings, and recommendations for purity monitoring and report for future ^{15}N-labeled research

Among the confirmed residues, nitrogen oxides ($^{15}NO_x$), $^{14}N^{15}N$ and $^{15}NH_3$ impurities deserve special attention. $^{15}NO_x$ is known to be easily reduced or oxidized thermochemically, photochemically, or electrochemically. These $^{15}NO_x$, $^{14}N^{15}N$ and $^{15}NH_3$ residues can be co-reacted alongside the dominant $^{15}N_2$ or $^{15}NH_3$

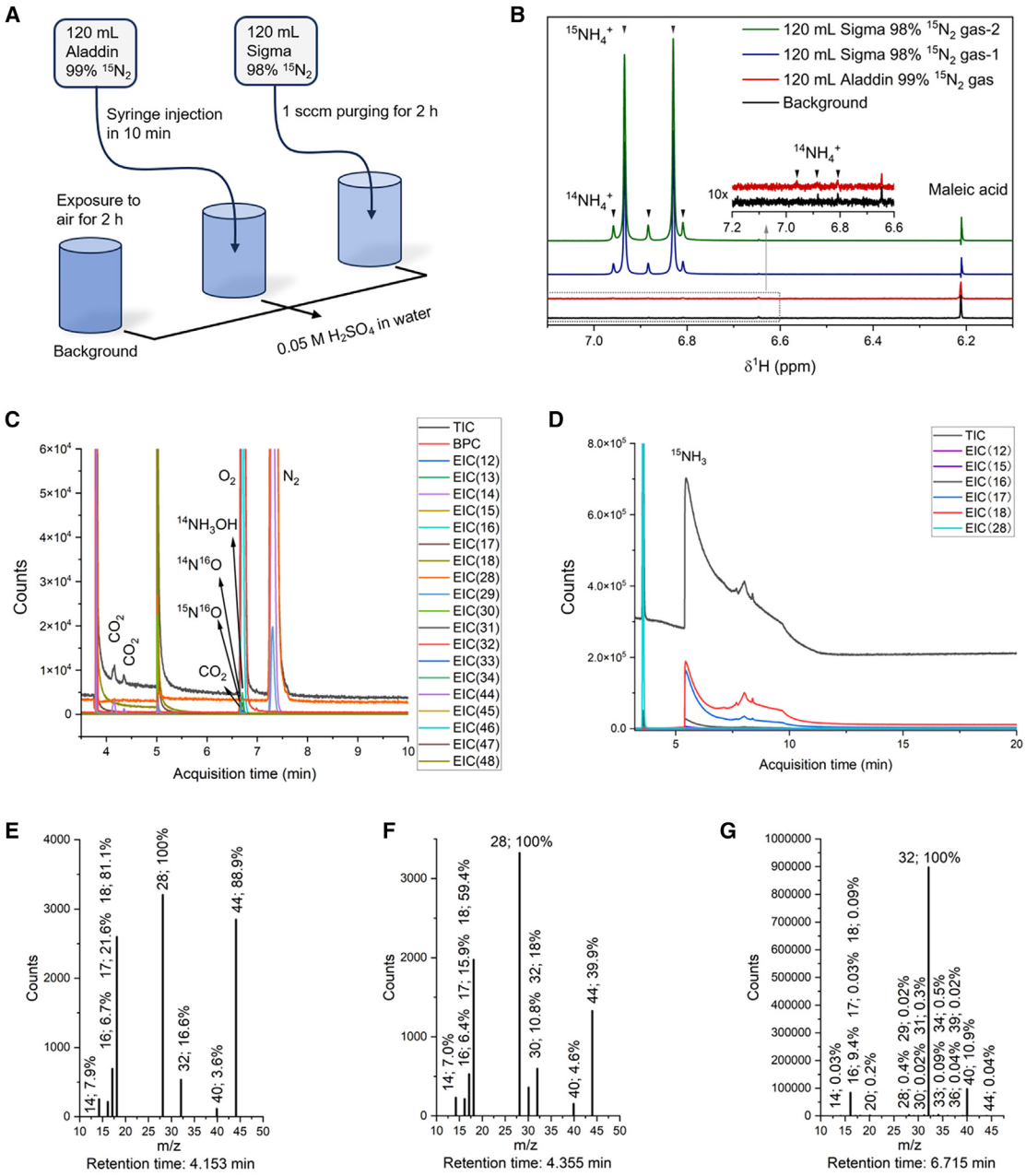

Figure 3. Analyses of ammonia residues and cylinder gas via ^{1}H-NMR and GC-MS

(A and B) (A) Schematic of the residual ammonia absorption using diluted H_2SO_4 solution, followed by (B) $^{14}NH_4^+$ and $^{15}NH_4^+$ quantifications using ^{1}H-NMR. The two spectra of Sigma 98% $^{15}N_2$ are obtained in the first and second 2 h after purging through 0.05 M H_2SO_4 absorbing solutions, respectively.

(C–G) TIC, BPC, and EIC spectra using (C) the *C1* method and (D) the *Cn* method, and corresponding MS patterns at the retention time of 4.2 (E), 4.4 (F), and 6.7 (G) min using the *C1* method.

gases and may be the origin for "unexpected" ^{15}N in previous $^{15}N_2$-labeling experiments.

For example, if a huge amount of Sigma 98%–99% $^{15}N_2$ cylinder gas was injected into a N_2 reduction system, detected $^{15}NH_3/^{15}NH_4^+$ product may be generated via the reduction $^{15}NO_x$ or the residual $^{15}NH_3$ even if the $^{15}N_2$ was not transformed. Without accounting for these ^{15}N-residues, any researcher would blindly believe that the observed $^{15}NH_3$ was solely from $^{15}N_2$ reduction.

$^{14}N^{15}N$ impurities affect nitrogen-cycle related studies in a totally different way. For example, if commercial $^{15}N_2$ cylinder gas is injected to investigate nitrogen atom exchange with ^{14}N-nitride materials or ^{14}N-gases, products containing ^{14}N from the cylinder gas could be erroneously interpreted to originate

Table 1. Comparison of the results of this study with the supplier's certificates

Entry	Supplier certificate[a] 99% Sigma $^{15}N_2$	GC-MS result 99% Sigma $^{15}N_2$	Supplier certificate[b] 98% Sigma $^{15}N_2$	GC-MS result 1L l 5L 98% Sigma $^{15}N_2$	GC-MS result[c] 99% Aladdin $^{15}N_2$	Entry	Supplier certificate[d] 98% Sigma $^{15}NH_3$	GC-MS result 98% Sigma $^{15}NH_3$
CO	23 ppm	ND	NM	ND	ND	Air	497 ppm	/
CO_2	76 ppm	55 ppm	<15 ppm	23 l 10 ppm	Trace	CO_2	<15 ppm	2 ppm
H_2	27 ppm	/	NM	/	/	CH_4 C_2H_6	<45 ppm	ND
$^{15}NH_3$[e]	NM	/	NM	/l 2,472–4,891 ppm	ND	N_2O	<15 ppm	Trace
$^{14}NH_3$[e]	NM	/	NM	/l 108–319 ppm	3	$^{14}N^{16}O$	NM	Trace[i]
O_2 (Ar)	81 ppm	/	32 ppm	/	/	$^{15}N^{16}O$	NM	30 ppm
C_2H_6	NM	ND	<15 ppm	ND	ND	–	–	–
$^{14}N^{16}O_2$	NM	231 ppm	<15 ppm	8 l 9 ppm	Trace	–	–	–
$^{15}N^{16}O_2$[f]	NM	176 ppm	NM	ND	ND	–	–	–
$^{14}N^{15}N$	NM	808 ppm	NM	9,608 l 6,653 ppm	16,252 ppm	–	–	–
$^{14}N^{15}N^{16}O$[g]	NM	$0.9A_{(NO2)}$	NM	$30.3A_{(NO2)}$ l $27.6A_{(NO2)}$	ND	–	–	–
NO[h]	0.3 ppm	$^{15}N^{16}O$ 501 ppm	NM	$^{15}N^{16}O$ 566 l 555 ppm	ND	–	–	–

NM = not mentioned; ND = not detected; / is N/A for the GC-MS method.
[a]Released on 12 February 2021, product number: 917540.
[b]Released on 19 July 2023, product number: 364584.
[c]No available certificate, product number: N117731. Residues were not quantified via standard curves due to the manual sampling.
[d]Released on 30 May 2023, product number: 299227.
[e]Quantified by the ^{1}H-NMR with calibration curve.
[f]Quantified by EIC m/z = 47 using the $^{14}NO_2$ calibration curve.
[g]The data represents the peak area of $^{14}N^{15}N^{16}O$ m/z = 45 relative to the peak area of $^{15}N^{16}O_2$ m/z = 47 ($A_{(NO2)}$), which is an area ratio instead of a direct concentration due to the lack of N_2O standard gas cylinder currently.
[h]Quantified by the EIC m/z = 31 using the $^{14}N^{16}O$ calibration curve.
[i]The EIC m/z = 30 can be alternatively induced by $^{15}N^{15}N$ and thus the $^{14}N^{16}O$ is not quantified.

from the nitride material or the exchanged ^{14}N-gases even such reactions did not occur. Furthermore, if commercial $^{15}N_2$ gas is used to investigate N_2 adsorption or binding, the $^{14}N^{15}N$ will show spectral features distinct to that of $^{15}N_2$. This will greatly affect the interpretation of vast results obtained in previous surface chemistry and coordination chemistry considering the relatively high concentration of $^{14}N^{15}N$ of 808–16,252 ppm.

Problems related to the impact of $^{15}NO_x$, $^{14}N^{15}N$ and $^{15}NH_3$ impurities are often obscured in literature due to the lack of reports on gas purity, injection amounts into detectors, and conversion of isotopic gases. In addition, we found that residues changed with time after comparing the suppliers' certifications for the same ^{15}N-cylinder gas over the course of approximately three years (Sigma 98% $^{15}N_2$). Yet, none of the certifications covered all ^{15}N- and ^{14}N-enriched residues compared with our results. In addition, previous studies also suggest that ^{15}N-cylinders from different production plants and distributors have different residual levels, and reported $^{15}NO_x$ and $^{15}NH_3$ impurities are typically within the range of 0.9–529 and 34–2,460 ppm, respectively.[13,17,18] In comparison, our results are within these reported residue levels, except for the previously undetected $^{14}N^{15}N$ of the highest concentration (808–16,252 ppm) among all N-residues and the much higher concentration of $^{15}NH_3$ (2,472–4,891 ppm). Notably, our results differ significantly with recent reports but agree well with the pioneer work in 2014. This comparison suggests that we may bought cylinders from same origins of those alerted in 2014, and the quality of different batches or origins differ significantly. Therefore, we emphasize that constant residue monitoring is necessary when using these commercial cylinder gases in isotope-labeling experiments.

Based on the aforementioned discussion, the most rigorous ^{15}N-labeling experiments should include (1) identification of residues in the ^{15}N-cylinder gas, (2) the trapping/removal of gaseous residues, (3) quantification of both reactants and products, and (4) comparison between the isotope-labeled performance indicators, such as conversion, activity, and selectivity, with that of ^{14}N-fed activity tests. Though these additional steps would require much more efforts, the results of this study have shown these precautions enhance the understanding, accuracy, reliability, and reproducibility of experiments.

Without knowledge of exact residues in commercial ^{15}N gases, targets are incomplete even for the most rigorous method advocated in previous studies—designing an pre-treatment setup for the selective removal of $^{14/15}NO_x$, $^{14/15}NH_3$, and air residues by catalysts (such as Cu), sorbents (such as molecular sieves), and/or a high-end commercial NO_x-NH_3 gas purifier before activity tests,[10,19,20] as indicated by the 1→6→3→4→7 protocol in Figure 4; the previously unrecognized residue like $^{14}N^{15}N$ was not excluded.[21] Only after the direct identification and quantification of residues in commercial ^{15}N-cylinder gases

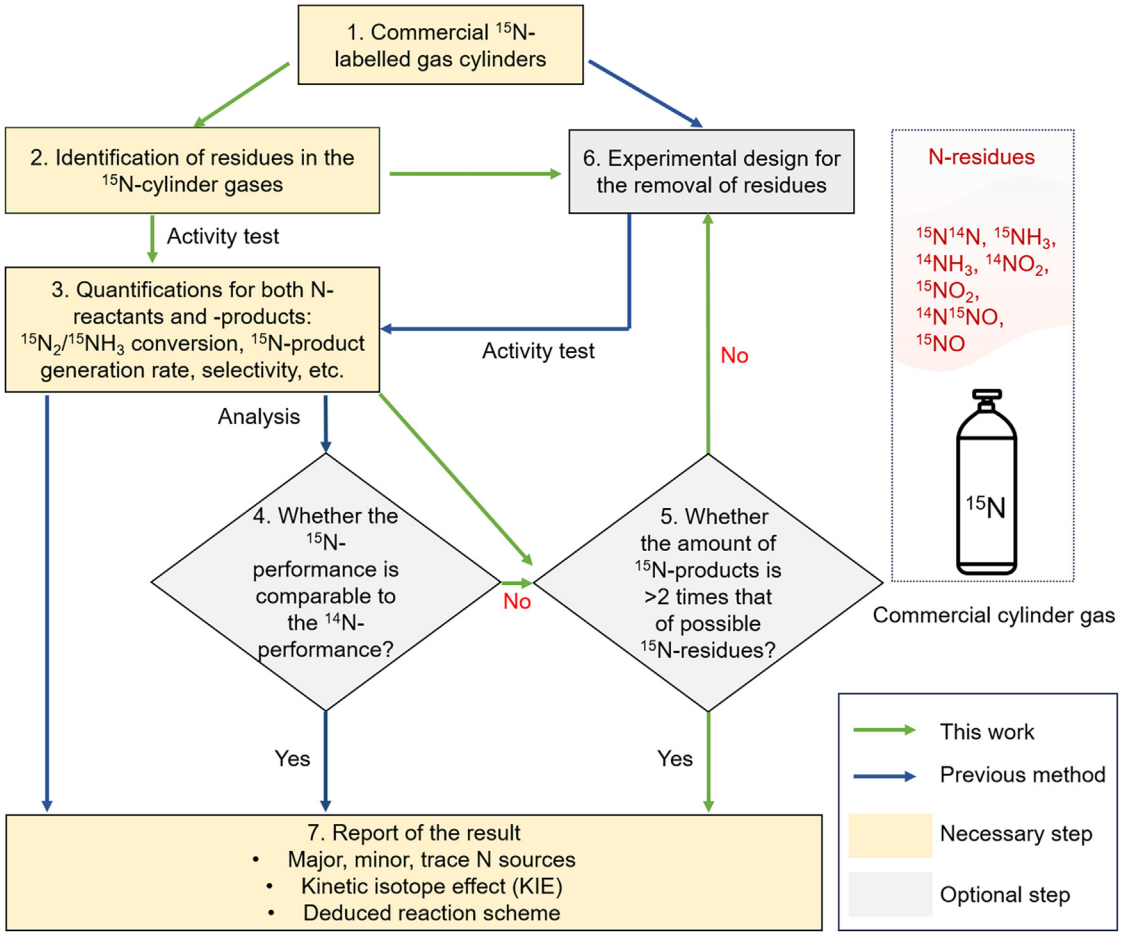

Figure 4. Suggested combination of protocols for future ^{15}N-labeling experiments

While the 1→6→3→4→7 protocol was previously advocated, in this work we highlight the potential of 1→2→3→(4)→5→7, 1→2→6→(2)→3→7, or 1→2→3→4→5→6→3→4→(5)→7 as an alternative protocol for the handling of ^{15}N-cylinders.

by this work can protocols 1→6→3→4→7, 1→2→3→(4)→5→7, 1→2→6→(2)→3→7, or 1→2→3→4→5→6→3→4→(5)→7 be employed with high confidence (Figure 4). Furthermore, based on all residues detected in previous studies and this work, isotope experiments cannot only be done at a single data point if a thorough removal of all residues cannot be ensured (as in most cases in current laboratorial N-related ammonia and urea studies),[21] and the amount of ammonia synthesized should be ideally similar regardless of using $^{14}N_2$ or $^{15}N_2$ (Step 4 in Figure 4). Data points of an ammonia/urea test should be recorded over time and varied reaction parameters such as temperature/overpotential/light intensity using $^{14}N_2$ or $^{15}N_2$ in thermo-, electro-, and photo-driven reactions.

Finally, we advocate a cost-efficient protocol, 1→2→3→5→7, to handle further ^{15}N-experiments based on our results and all the ^{15}N-results reported so far (Figure 4). In previous 1→6→3→4→7 protocol advocated, of which the key is whether the ^{15}N-experiment can yield comparable performance to the unlabeled ^{14}N-experiment, with the conversion of the ^{15}N feed, selectivity and rate, highlighted in step 4 in Figure 4. If their performance indicators are similar, this protocol requires no additional setups or procedures. However, as we have identified so many unexpected residues in commercial ^{15}N-cylinder gases, the requirements for step 6—gas pre-treatment, especially in experimental setup, should be compilated that cannot be accessed by most laboratories. Under this circumstance, the protocol 1→2→3→5→7 requires no gas pre-treatment setup, with the steps 2, 3, and 5 highlighted, is of vital importance to the community. To amplify, at a certain reaction time with a known gas flow rate, the volume of gas flowing through the reactor is known. Thus, the maximum amount of ammonia produced by the impurities can be calculated assuming that all impurities are converted to NH_3, urea, or any targeted N-products based on steps 2 and 3—identification and quantification of impurities in commercial cylinder gas. Then this calculated maximum amount of N-product from impurity can be compared with the amount of N-residues obtained experimentally. If the experimentally obtained ^{15}N-product is more than two times greater than the amount of all possible fed ^{15}N-residues, it requires no additional procedures to confirm the reaction of ^{15}N-reactant. Specifically, the chosen baseline of >2 concentration between of ^{15}N products to total possible ^{15}N residues was adopted from the instrumental analytic chemistry, where the signal to noise ratio

should exceed 2 to identify a targeted species. We believe that this alternative protocol can especially save time and effort for any future ammonia and urea studies, and its establishment is not possible without the joint effort of the community. Noteworthily, this protocol can foresee its limitation in reactions where the concentration of targeted ^{15}N-product is lower than 2× the concentration of all N-residues.

Limitations of the study

Concentrations of the $^{14}N^{15}N^{16}O$ impurity are not quantified in all cylinders due to the lack of standard gas cylinders, while their relative peak areas to that of NO_2 have been recorded, which can be translated into an estimated concentrations using the relative response factor of N_2O to NO_2 in MS. Due to the high cost of ^{15}N-gas, this study only sampled several selected cylinders that are commercially available in China and North America. Despite this, the exceptionally high concentrations of impurities discovered in this study sufficiently alert the global community.

RESOURCE AVAILABILITY

Lead contact

Further information and requests for resources should be directed to and will be fulfilled by the lead contact, Geoffrey Ozin (g.ozin@utoronto.ca). Chengliang Mao (chengliang.mao@mail.utoronto.ca

Materials availability

This study did not generate new unique reagents.

Data and code availability

This study did not generate any datasets.

- All data reported in this paper will be shared by the lead contact upon reasonable request.
- This paper does not report original code.
- Any additional information required to reanalyze the data reported in this paper is available from the lead contact upon reasonable request.

ACKNOWLEDGMENTS

This work is supported by and National Key Research and Development Program of China (2022YFB4003900), National Natural Science Foundation of China (NSFC; 52206284), and Natural Sciences and Engineering Research Council of Canada (NSERC) and Greg Vezina of Hydrofuel Canada Inc. The authors acknowledge Dr. Sherry Dai and Dr. Darcy Burns at the University of Toronto CSICOMP NMR Facility for conducting NMR measurements.

AUTHOR CONTRIBUTIONS

S.T., conceptualization, data curation, funding acquisition, methodology, resources, validation, visualization, writing – original draft, writing – review & editing. C.M., conceptualization, data curation, funding acquisition, investigation, methodology, project administration, resources, validation, writing – original draft, writing – review & editing. G.Z., data curation, validation, visualization. J.Y., methodology, investigation, validation. W.Q., methodology, data curation, resources. L.W., investigation, data curation, resources. G.O., conceptualization, funding acquisition, project administration, resources, supervision.

DECLARATION OF INTERESTS

The authors declare no competing interests.

STAR★METHODS

Detailed methods are provided in the online version of this paper and include the following:

- KEY RESOURCES TABLE
- METHOD DETAILS
  - Selection of ^{15}N- and standard-gas cylinders
  - Procedures and detection parameters, sampling methods, and data analysis
- QUANTIFICATION AND STATISTICAL ANALYSIS

SUPPLEMENTAL INFORMATION

Supplemental information can be found online at https://doi.org/10.1016/j.isci.2025.112072.

Received: April 1, 2024
Revised: January 3, 2025
Accepted: February 17, 2025
Published: February 20, 2025

REFERENCES

1. Mao, C., Byun, J., MacLeod, H.W., Maravelias, C.T., and Ozin, G.A. (2024). Green Urea Production for Sustainable Agriculture. Joule *8*, 1224–1238.
2. Chen, J.G., Crooks, R.M., Seefeldt, L.C., Bren, K.L., Bullock, R.M., Darensbourg, M.Y., Holland, P.L., Hoffman, B., Janik, M.J., Jones, A.K., et al. (2018). Beyond fossil fuel–driven nitrogen transformations. Science *360*, eaar6611.
3. Schlögl, R. (2003). Catalytic Synthesis of Ammonia—A "Never-Ending Story"? Angew. Chem. Int. Ed. *42*, 2004–2008.
4. Mao, C., Li, H., Gu, H., Wang, J., Zou, Y., Qi, G., Xu, J., Deng, F., Shen, W., Li, J., et al. (2019). Beyond the Thermal Equilibrium Limit of Ammonia Synthesis with Dual Temperature Zone Catalyst Powered by Solar Light. Chem *5*, 2702–2717.
5. Xia, M., Mao, C., Gu, A., Tountas, A.A., Qiu, C., Wood, T.E., Li, Y.F., Ulmer, U., Xu, Y., Viasus, C.J., et al. (2022). Solar urea: towards a sustainable fertilizer industry. Angew. Chem. Int. Ed. *61*, e202110158.
6. Mao, C., Wang, J., Zou, Y., Shi, Y., Viasus, C.J., Loh, J.Y.Y., Xia, M., Ji, S., Li, M., Shang, H., et al. (2023). Photochemical Acceleration of Ammonia Production by Pt_1-Pt_n-TiN Reduction and N_2 Activation. J. Am. Chem. Soc. *145*, 13134–13146.
7. (2024). Atomic Weight of Nitrogen | Commission on Isotopic Abundances and Atomic Weights. https://ciaaw.org/nitrogen.htm.
8. Andersen, S.Z., Čolić, V., Yang, S., Schwalbe, J.A., Nielander, A.C., McEnaney, J.M., Enemark-Rasmussen, K., Baker, J.G., Singh, A.R., Rohr, B.A., et al. (2019). A rigorous electrochemical ammonia synthesis protocol with quantitative isotope measurements. Nature *570*, 504–508.
9. Suryanto, B.H.R., Du, H.-L., Wang, D., Chen, J., Simonov, A.N., and MacFarlane, D.R. (2019). Challenges and prospects in the catalysis of electroreduction of nitrogen to ammonia. Nat. Catal. *2*, 290–296.
10. Dabundo, R., Lehmann, M.F., Treibergs, L., Tobias, C.R., Altabet, M.A., Moisander, P.H., and Granger, J. (2014). The contamination of commercial $^{15}N_2$ gas stocks with ^{15}N–labeled nitrate and ammonium and consequences for nitrogen fixation measurements. PLoS One *9*, e110335.
11. Diocares, R., Morey, T., and Holguin, G. (2006). Producing and dispensing small quantities of $^{15}N_2$ gas at atmospheric pressure. Anal. Biochem. *352*, 302–304.
12. Wood, C.C., and Kennedy, I.R. (2001). A simple, handheld apparatus for generating small volumes of $^{15}N_2$ from ^{15}N-labeled ammonium salts. Anal. Biochem. *296*, 147–149.
13. De Ras, M., Hollevoet, L., Martens, J.A., Liu, T., Nicolai, B.M., Hertog, M.L.A.T.M., Hofkens, J., and Roeffaers, M.B.J. (2024). Beyond acceptable

limits: intrinsic contamination in commercial $^{15}N_2$ impedes reliable N_2 reduction experiments. Green Chem. *26*, 1302–1305.

14. NIST Standard Reference Database 69: NIST Chemistry WebBook.
15. Choi, J., Suryanto, B.H.R., Wang, D., Du, H.-L., Hodgetts, R.Y., Ferrero Vallana, F.M., MacFarlane, D.R., and Simonov, A.N. (2020). Identification and elimination of false positives in electrochemical nitrogen reduction studies. Nat. Commun. *11*, 5546.
16. Li, K., Li, S., Zhou, Y., Andersen, S.Z., Saccoccio, M., Sazinas, R., Bruun Pedersen, J., Fu, X., Chakraborty, D., Vesborg, P., et al. (2022). Increasing Ammonia Formation Rates of Li-Mediated Ammonia Synthesis with High Surface Area Copper Electrodes. Science *374*, 1593–1597.
17. Fu, X., Pedersen, J.B., Zhou, Y., Saccoccio, M., Li, S., Sažinas, R., Li, K., Andersen, S.Z., Xu, A., Deissler, N.H., et al. (2023). Continuous-flow electrosynthesis of ammonia by nitrogen reduction and hydrogen oxidation. Science *379*, 707–712.
18. Kibsgaard, J., Nørskov, J.K., and Chorkendorff, I. (2019). The Difficulty of Proving Electrochemical Ammonia Synthesis. ACS Energy Lett. *4*, 2986–2988.
19. Zhao, Y., Shi, R., Bian, X., Zhou, C., Zhao, Y., Zhang, S., Wu, F., Waterhouse, G.I.N., Wu, L.Z., Tung, C.H., and Zhang, T. (2019). Ammonia detection methods in photocatalytic and electrocatalytic experiments: how to improve the reliability of NH_3 production rates? Adv. Sci. *6*, 1802109.
20. Iriawan, H., Andersen, S.Z., Zhang, X., Comer, B.M., Barrio, J., Chen, P., Medford, A.J., Stephens, I.E., Chorkendorff, I., and Shao-Horn, Y. (2021). Methods for nitrogen activation by reduction and oxidation. Nat. Rev. Methods Primers *1*, 1–26.
21. Ye, T.-N., Park, S.-W., Lu, Y., Li, J., Sasase, M., Kitano, M., Tada, T., and Hosono, H. (2020). Vacancy-enabled N_2 activation for ammonia synthesis on an Ni-loaded catalyst. Nature *583*, 391–395.

STAR★METHODS

KEY RESOURCES TABLE

REAGENT or RESOURCE	SOURCE	IDENTIFIER
Chemicals, peptides, and recombinant proteins		
$^{15}NH_3$, ^{15}N > 98 atom%, 1 L	MilliporeSigma Canada LTD	299227
$^{15}N_2$, ^{15}N > 98 atom%, 1 L	MilliporeSigma Canada LTD	364584
$^{15}N_2$, ^{15}N > 98 atom%, 5 L	MilliporeSigma Canada LTD	364584
$^{15}N_2$, ^{15}N > 99 atom%, 1 L	MilliporeSigma Canada LTD	917540
$^{15}N_2$, ^{15}N > 99 atom%, 1 L	Shanghai Aladdin Biochemical Technology Co., Ltd.	N117731
Other		
GC-MS	Agilent Technologies, Inc.	7890B
MestReNova software	Mestrelab Research S.L.	15.0.0–34764

METHOD DETAILS

Selection of ^{15}N- and standard-gas cylinders

Sigma $^{15}N_2$ cylinders are most available in North America. However, they were found to contain ^{15}N-enriched nitrogen residues, including nitrate, nitrite and/or ammonium in equilibrating solutions, by Dabundo and co-workers in 2014.[1] Despite the authors' indication that they had contacted the supplier to enhance the purity of $^{15}N_2$ products, the identities of the residues in the cylinders have not been well understood since. Therefore, we focus on Sigma cylinders of different purities, including Sigma 98% $^{15}N_2$ 1L (364584; PCode: 1003641588) and 5L (364584; PCode: 1003641585) cylinders, and Sigma 99% $^{15}N_2$ 1L (917540, PCode: 1003411220) cylinder, as well as a previously unchecked Sigma 99% $^{15}NH_3$ 1L (299227; PCode: 1003630202) cylinder. These isotope gases were all packed in 0.46 L cylinders, which were then connected to the in-line batch-mode GC-MS system via a vacuum injection line. In addition, Aladdin is the major $^{15}N_2$ (99% $^{15}N_2$ 1L, N117731, lot #: A2218558) gas bag provider in China and was thus analyzed by a manual injection with a GC syringe.

Standard gases include a mixed-hydrocarbons (503 ppm butane, 523 ppm ethane, 523 ppm ethylene, 506 ppm n-hexane, 523 ppm methane, 510 ppm n-pentane, 540 ppm propane, 515 ppm propylene balanced by Ar), a mixed CO-CO_2-CH_4 (5000 ppm CO_2, 5000 ppm CH_4, 5000 ppm CO balanced by Ar), a diluted NO_2 (101 ppm NO_2 balanced by Ar), a diluted NO (100 ppm NO balanced by Ar), and 5.0 purity Ar and He, which were obtained from Praxair.

Procedures and detection parameters, sampling methods, and data analysis

All measurements were conducted using an Agilent 7890B GC-MS (electron ionization source) equipped with five capillary columns (HP-PLOT Molesieve, 19091P-MS4E, 30 m × 0.320 mm x 12 mm; HP-PLOT Q PT, 19091P-QO3PT, 15 m × 0.320 mm x 20 mm; DB-FFAP, 123–3212, 15 m × 0.320 mm x 0.25 mm; 160-2625-5, FST 0.15 mm × 5 m; 160-2615-5, FST 0.18 mm × 5 m) using 5.0 purity He carrier gas and 5.0 purity Ar purge gas. Here two methods were used for the detection of possible gaseous residues in commercial cylinders. The first oven temperature program, termed *C1* method, held 30°C for 14 min for the detection of CO_2, CO, N_2, O_2, NO, NO_2, CO and CH_4. The second program, termed *Cn* method, held 40°C for 4 min, ramped at 20°C/min to 180°C, and then held 180°C for 14 min for the detection of NH_3 and hydrocarbons. Prior to each measurement, the gas line was evacuated overnight and the GC columns were baked at 140°C overnight to minimize contaminations and increase separation capability.

After calibrating the GC-MS with standard gas cylinders, targeted ^{15}N-cylinder gases were injected through a home-made vacuum injection line (Scheme 1). Within this vacuum system, all connections and valves were obtained from the Swagelok Vacuum Series. The in-line digital pressure indicator was obtained from Omega. The volume of the gas transfer line was 21.5 mL, as determined by the ideal gas law using a fixed-volume reactor (12.0 mL; measured via water pre-filling). Gas injection method: Valves 1 and 7 in Scheme 1 were closed while valves 2–6 were opened to allow the evacuation of the gas plumbing to −14.6 to −14.7 psi. Then valve 6 was closed, and valves 1 was opened and tuned to fill the gas plumbing with ambient-pressure (0 psi) sample gas, followed by immediate gas inlet with auto-sampling valves embedded in the GC-MS. In some occasions, the in-line gas pressure was first controlled to −1 to −4 psi by the inlet of standard NO_2 cylinder gas (replacing the ^{15}N cylinder with the NO_2 cylinder in Scheme 1), followed by opening the valve to air to make the pressure to 0 psi and then closing the valve immediately. Notably, the Aladdin $^{15}N_2$ was packed in a gas bag with a rubber septum which was not compatible with our Swagelok connections, and thus it

was sampled by manual GC syringe injection. Control and background spectra were respectively obtained under air (0 psi) and vacuum (−14.6 to −14.7 psi) before the measurements of cylinder gases to identity possible background contaminations and air leaking.

Each cylinder gas was analyzed for at least three separate runs to confirm any detected residues. The obtained sample GC spectra were first compared with control and background spectra to identify effluents from the sampled cylinders. To amplify, background spectra were collected without the sampled gas, i.e., keeping the gas transfer line under vacuum when sampling, which showed a weak $^{14}N_2$ peak at the retention time of 6.8 min, as well as the O_2 peak at 6.7 min and two mixed air peaks at 3.8 and 5.6 min using the *C1* method (Figure S4). The $^{14}N_2$ and O_2 peaks originated from the residual air in the gas system of the GC, while the two air peaks were attributed to leaks induced by the gas sampling valves moving between on/off resulting in a transient pressure change in the MS detector vacuum system. These residues and MS air leaks are usually inevitable in a GC-MS system. Noteworthily, these N_2/O_2 residues in GC will make the quantification of N_2/O_2 contents in sampled gases unreliable, while the transient leaks in MS do not affect our detection of possible CO_2, NO_x, NH_3, H_2O even they present in the ambient air. This is because the air leak only occurs in the MS part and do no enter the GC system. Therefore, the leaked air will be degassed immediately by the dual vacuum pumps connected to the MS to re-balance the pressure of the vacuum system, and thus cannot be separated and injected to the MS detector in a time-resolved fashion as the case for conventional gas sampling via the GC inlet. This is revealed by the fast decay of the two valve-on/off composite peaks and the lack of the air-component CO_2 at 4.2 min in the control spectra. Background spectra using the *Cn* method was collected in the same way. Within the spectra for the standard gaseous gas cylinder, CO_2 (4.1 min), NO_2 (4.3 min), NH_3 (5.4 min), C_2H_4 (4.7 min), C_2H_6 (5.2 min), C_3H_6 (8.1 min), C_3H_8 (8.3 min), C_4H_{10} (10.8 min), C_5H_{12} (13.0 min), and C_6H_{12} (16.5 min) hydrocarbons could be detected besides the balance Ar that showed a strong peak at 3.6 min (Figure S3).

Then the retention time-dependent TIC, BPC, and extracted ion chromatograms (EIC; such as m/z = 12, 13, 14, 15, 16, 17, 18, 28, 29, 30, 31, 32, 40, 44, 45, 46, 47, and 48) MS spectra were monitored to analyze ionized molecules. Subsequently, thorough analyses were conducted by comparing obtained MS patterns with that of deduced standard substances such as N_2, NO, NO_2, CO_2, CO, CH_4, H_2O, O_2, Ar, and NH_3. At last, confirmed NO_x residues (including their isotopes) were quantified by NO and NO_2 standard curves. Specifically, the concentration of $^{14}N^{15}N$ is calculated via:

$$^{14}N^{15}N\ \% = \frac{I(^{14}N^{15}N) - I(^{14}N_2)/100}{I(^{15}N_2)} * 100\% \quad \text{(Equation 1)}$$

where $I(^{14}N^{15}N)$, $I(^{14}N_2)$, $I(^{15}N_2)$ represent the peak area of the m/z = 29, 28, and 30 EIC spectra, respectively. The 1/100 of $I(^{14}N_2)$ represents the peak area originating from the residual $^{14}N_2$ gas (natural abundance) in the GC-MS system instead of the $^{14}N^{15}N$ contaminant in the $^{15}N_2$ cylinder gas.

The concentration of NO_x was calculated using a standard curve method based on the NO and NO_2 diluted by Ar standard cylinder gas. Notably, we observed several unconventional phenomena during the in-line GC-MS quantification of NO_2, which may be important for the reproducibility of the result reported herein (Figure S5). First, the NO_2 preferentially co-eluted with Ar to show peaks at the retention time of 6.6 min, which differed with the 4.4 min observed for the co-eluted NO_x residues with CO_2 in commercial ^{15}N-cylinder gases. Even with the co-injection of 1—4 psi air (with ~420 ppm CO_2), the retention time maintained at 6.6 min. Second, the peaks at 6.6 min include m/z = 46 and 47, and 48 of similar intensities, which are likely the $^{14}NO_2$, $H^{14}NO_2$, and $H_2{}^{14}NO_2$, respectively. All three peak areas were integrated and summed up to correspond to the 101 ppm NO_2. Third, the m/z = 46, 47, and 48 peaks disappeared completely if the NO_2 in the gas plumbing was sampled more than once. To amplify, around 25 mL 101 ppm NO_2 was stored in the inlet gas plumbing before the GC-MS sampling. This gas could yield NO_x peaks at 6.6 min in the GC-MS spectrum when sampled the first time, while sampling the rest gas could not observe any NO_x peaks in the GC-MS spectra. This was not induced by the leaking or oxidation of NO_x by air as co-inlet of air would not affect the detection of NO_x. Therefore, we deduce that NO_2 may strongly adsorb on or even reacted with the interior wall of the stainless-steel gas pipe line and pressure gauge, which can go to completion within merely 14 min. These three points merit particular caution for any future studies that intend to reproduce the methodology of this work. Specifically, the retention time for $^{15}N^{16}O$ (m/z = 31) and $^{14}N^{15}N^{16}O$ (m/z = 45) are the same (7.2 min), indicating the potential contribution of m/z = 31 from the fragment of $^{14}N^{15}N^{16}O$ molecule (Figure S6). To accurately quantify the $^{15}N^{16}O$ concentration, the fragment portion of m/z = 31 is excluded via:

$$I_{Real}\left(^{15}N^{16}O\right) = I_{Total}\left(^{15}N^{16}O\right) - 0.158 * I(^{15}N^{14}NO) \quad \text{(Equation 2)}$$

where I_{total} and $I_{^{14}N^{15}N\,O}$ are signal intensity of m/z = 31 and m/z = 45, respectively, and 0.158 is the theoretic intensity ratio between m/z = 31 fragment and m/z = 45 for the $^{14}N^{15}N^{16}O$ molecule.

The residual ammonia in commercial gas cylinder or gas was first absorbed by H_2SO_4 solution and then quantified by ^{1}H-NMR using the maleic acid and DMSO-d_6 as the internal standard and locking solvent, respectively, with the background $^{14}NH_3$ disregarded. Specifically, the 5 L 98%-purity Sigma $^{15}N_2$ cylinder gas was purged through a 0.05 M H_2SO_4 absorbing solution of known volume (typically 0.95 mL) at a flow rate of 1 sccm for 120 min (totaling 120 mL $^{15}N_2$) using the same vacuum pre-cleaned gas plumbing. Differently, 120 mL 99%-purity Aladdin $^{15}N_2$ was extracted via a syringe from the rubber septum of the gas bag, and then injected into a 0.05 M H_2SO_4 absorbing solution manually in 10 min. Then 50 mL 1 mM Maleic acid, 50 mL DMSO-d_6 (sometimes 110 mL was used) were added into the 950 mL absorbing solution. After thorough mixing by shaking, 600 mL of above solution was

added into a 5 mm tube for ^{1}H-NMR measurements via a Bruker 700 MHz spectrometer. The standard curve for the NH_4^+ quantification using the ^{1}H-NMR was y = 0.011 + 0.174x, where y and x represent the normalized peak area of ammonia (through assigning the peak area of the internal standard maleic acid in all NMR spectra as 1) and ammonia concentration in solution (mg/L or ppm).

QUANTIFICATION AND STATISTICAL ANALYSIS

Statistical analyses of data were performed using Agilent Qualitative Navigator, MestReNova, and Excel software.